Biopress Journal of Advanced Pharmacology Vol.2 Issue. 9 (2026)

Targeting Mpox with Natural Products: In Silico Discovery of DNA Topoisomerase 1B Inhibitors

Tanya Jindal[1*], Isha Thakur[1], Puneet[2*], Gurinder Singh[1], Kavita Rana[1]

[1] Rapture Biotech Pvt. Ltd., Mohali, Punjab, India

[2]Assistant Professor, Central Instrumentation Facility and Research and Development Cell, Lovely Professional University, Phagwara, Punjab.

Corresponding author: tanya.jindal2611@gmail.com, drpuneetabajajphd@gmail.com

Doi: https://doi.org/10.5281/zenodo.23613326

Received: September 12 2026

Accepted: 24 September 2026

Abstract

Mpox remains a public health concern, and the two drugs in clinical use are already limited by resistance or by dose-related toxicity. Viral DNA topoisomerase 1B (Topo 1B) is an alternative target: the enzyme is required for orthopoxvirus replication and shares less than 45 % sequence identity with its human counterpart. No experimental structure of the mpox enzyme has been deposited, so we built a homology model from vaccinia and variola templates (GMQE 0.94; QMEANDisCo 0.86 ± 0.05) and validated it on the SAVES v6.1 portal, where 95.5 % of residues fell in favoured Ramachandran regions and the ERRAT quality factor reached 95.1 %. We then docked 1,353 phytochemicals, curated from 16 Indian medicinal plants in the IMPPAT 2.0 atlas, into the top-ranked pocket with AutoDock Vina 1.2.5 running under PyRx. One hundred and thirteen compounds, 8 % of the library, scored at or below −9.0 kcal/mol and so outperformed the coumarin reference inhibitor novobiocin (−8.8 kcal/mol) redocked under identical settings. Sequential filtering in SwissADME and ADMETlab 3.0 narrowed these to seven compounds that satisfied the Lipinski and Veber rules and carried no predicted hERG, cytochrome P450 or acute-toxicity liability. Five of the seven are withanolides from *Withania somnifera*. Withasomidienone (IMPHY000630) returned the best score (−10.3 kcal/mol) but is predicted to be poorly soluble, so we advance Withanolide L (IMPHY009438, −10.2 kcal/mol) as the primary lead: it combines comparable affinity with moderate predicted solubility and no Lipinski violations. Its pose is held by hydrogen bonds to Lys167, Tyr136 and Tyr209 together with π-alkyl and van der Waals contacts. These results are computational predictions and now need enzymatic and cellular testing.

Keywords: Mpox; DNA topoisomerase 1B; Virtual screening; Molecular docking; Natural products; Withanolides; ADMET

1. Introduction

Mpox is caused by an orthopoxvirus first recovered from a human patient in 1970. The virus moved out of its historical African range in May 2022, and by 30 April 2025 the World Health Organization had recorded 142,151 PCR-confirmed infections and 328 deaths across 133 countries, with clade Ib still circulating in ten of them [1]. Routine smallpox vaccination stopped in 1980, which leaves roughly half the world population without cross-protective immunity and keeps the susceptible pool large.

Treatment options are thin. Tecovirimat acts on the viral F13 envelope protein, and F13L point mutants that reduce susceptibility — I372N and A290V among them — have appeared both in culture and in treated patients [2,3].

Brincidofovir, a lipid conjugate of cidofovir authorised for emergency use against mpox, ran into dose-related hepatotoxicity and gastrointestinal events in early clinical work [4,5]. Both agents act late in assembly and envelopment, so an antiviral working through an unrelated mechanism would be worth having even while the current drugs hold.

Viral DNA topoisomerase 1B offers one such mechanism. The enzyme relieves superhelical tension in the viral genome by forming a transient 3′-phosphotyrosyl bond with DNA, and deleting it or mutating its active site cripples vaccinia virus replication [6]. Identity with human Topo 1B stays below 45 %, which leaves room for selective inhibition. The coumarin antibiotic novobiocin established the principle three decades ago by inhibiting the vaccinia enzyme and lowering viral titres in cell culture, although its affinity and pharmacokinetics are modest [7]. No high-resolution mpox structure has been deposited. Homology models built on vaccinia and variola templates nonetheless agree on a catalytic pocket framed by Gly132, Lys133 and Tyr136, the residues that mutagenesis has repeatedly implicated in transesterification [8].

Plant metabolites are a reasonable place to look for chemistry against that pocket. Close to 60 % of licensed antivirals trace back to natural products or natural-product-inspired scaffolds [9], and the IMPPAT 2.0 atlas alone curates 17,967 phytochemicals from 4,010 Indian medicinal plants [10]. Compounds with a long record of human use also carry informal safety information that a synthetic library does not.

Docking provides a cheap triage ahead of assay work. AutoDock Vina holds its mean binding-energy error near 2–3 kcal/mol while scoring thousands of ligands [11], and the current PyRx release bundles Vina 1.2.5 with multithreaded exhaustiveness control, which brings a mid-sized natural-product screen within reach of a desktop machine [12,13]. SwissADME and ADMETlab 3.0 then return solubility, cytochrome P450, hERG and acute-toxicity flags in a single pass [14,15].

Computational work on mpox Topo 1B has so far been narrow. Hu and co-workers modelled the enzyme and screened a small compound set, but without a reference inhibitor or an ADMET stage [16]; published flavonoid-panel screens against mpox proteins left Topo 1B out of the target list altogether. We therefore curated 1,353 phytochemicals from 16 medicinal plants, built and validated a model of mpox Topo 1B, docked the whole library, benchmarked the scores against redocked novobiocin, and passed the survivors through a two-stage ADMET funnel. The sections below describe the pipeline and the shortlist it produced.

2. Materials and Methods

2.1 Plant selection and phytochemical library

Sixteen Indian medicinal plants with documented antiviral or immunomodulatory use were selected from the IMPPAT 2.0 atlas [10]. Table 1 lists them with the rationale for each. Every available three-dimensional SDF record was downloaded, giving 1,353 unique phytochemicals. No drug-likeness or oral-bioavailability filter was applied at this stage, so that historically used scaffolds which fall outside modern rule sets were not discarded before they had been docked.

Table 1. The 16 Indian medicinal plants used to build the screening library, with the reported activity that motivated their inclusion.

Plant species	Reported activity relevant to this screen
Phyllanthus acidus	Broad-spectrum antimicrobial activity; source of antioxidant compounds
Andrographis paniculata	Contains andrographolide, an antiviral and immunomodulatory diterpenoid
Glycyrrhiza glabra	Source of glycyrrhizin, a triterpenoid saponin with documented antiviral activity
Ocimum tenuiflorum	Traditional adaptogenic, antimicrobial and immunomodulatory use
Curcuma longa	Curcumin, with anti-inflammatory and antiviral activity

Withania somnifera	Withanolides with immunomodulatory and antiviral effects
Azadirachta indica	Limonoids with broad antiviral and antibacterial activity
Camellia sinensis	Catechins such as EGCG, reported to inhibit viral entry and replication
Melissa officinalis	Polyphenols active against herpes simplex and other viruses
Phyllanthus niruri	Traditional use in viral hepatitis; inhibition of viral polymerases
Tinospora sinensis	Alkaloids and diterpenoid lactones that modulate immune responses
Allium sativum	Organosulfur compounds, including allicin, with antiviral activity
Thuja occidentalis	Traditional use against viral infections and warts via immune stimulation
Sinopodophyllum hexandrum	Source of podophyllotoxin, an antiviral and antineoplastic lignan
Moringa oleifera	Flavonoids and glucosinolates with antiviral and anti-inflammatory reports
Berberis aristata	Berberine, with broad-spectrum antiviral activity

2.2 Homology modelling

Because no mpox DNA topoisomerase 1B crystal structure is available, the viral sequence (NCBI RefSeq YP_009352711) was submitted to the SWISS-MODEL server on 15 April 2025 [17]. Vaccinia and variola templates (PDB IDs 1A41, 3IGC and 2H7F) produced a hybrid model with a Global Model Quality Estimation (GMQE) of 0.94 and a QMEANDisCo global score of 0.86 ± 0.05.

2.3 Structural validation

Model quality was assessed on the SAVES v6.1 portal [18]. Stereochemistry was checked with PROCHECK, which placed 95.5 % of residues in favoured Ramachandran regions [19]. Agreement between the three-dimensional structure and its sequence was tested with VERIFY3D, where 84.35 % of residues scored ≥ 0.1 [20]. ERRAT returned an overall quality factor of 95.1 % [21]. All three metrics clear the conventional cut-offs for a model intended for docking.

2.4 Receptor preparation

The model was downloaded in PDB format and stripped of hetero-atoms and water in BIOVIA Discovery Studio 2025 [22]. Polar hydrogens were added and Gasteiger charges assigned in AutoDockTools 1.5.7, both of which the Vina scoring function requires [23].

2.5 Binding-site prediction

Ligandable pockets were predicted with PrankWeb/P2Rank [24]. The top-ranked site was carried forward, which confines the search to one pocket and keeps the screen tractable. Its residues are: Arg67, Gln69, Val77, Arg80, Asn81, Lys83, Arg84, Arg86, Ile87, Arg90, Phe127, Phe128, Ile129, Arg130, Phe131, Gly132, Lys133, Tyr136, Asn140, Thr142, Val143, Gly144, Phe164, Gly166, Lys167, Asp168, Lys169, His172, Phe174, Tyr209, Ile212, Arg218, Ile219, Lys220, Arg223, Thr224, Val263, Gly264, His265, Arg272, Ala273 and Tyr274.

2.6 Ligand preparation

SDF files were energy-minimised in PyRx 0.9.9 using Open Babel 3.1.1 with the MMFF94 force field over 500 steps, then converted to PDBQT [12,25]. Stereochemistry was left untouched and no pan-assay interference (PAINS) filter was applied, again to avoid removing scaffolds before they had been scored.

2.7 Molecular docking

AutoDock Vina 1.2.5 was run through the PyRx interface with exhaustiveness 8 and num_modes = 10 [11,13]. Vina estimates binding affinity from an empirical function that sums weighted steric, hydrogen-bond and hydrophobic terms and applies a penalty for rotatable bonds:

$$\Delta G_{binding} = \Sigma_{i,j}\, f(d_{i,j}) + c_{hbond}\, \Sigma_{H\text{-}bonds}\, g(\theta) + c_{hydrophobic}\, \Sigma_{hydrophobic\ contacts}\, h(d_{i,j}) + c_{rot}\, N_{rot}$$

The grid was a 20 Å cube centred at (29.2539, −11.0124, 26.5414), which encloses the catalytic residues Gly132, Lys133 and Tyr136 with room for the larger ligands in the library [26]. Each of the 1,353 ligands was docked once and allowed up to ten poses, giving 12,202 poses in total.

2.8 Reference inhibitor

Novobiocin (PubChem CID 54675784), a characterised orthopox Topo 1B inhibitor, was redocked under the same grid and exhaustiveness settings. Its best pose scored −8.8 kcal/mol and was used as the benchmark for the screen.

2.9 ADME and toxicity filtering

The 113 ligands scoring at or below −9.0 kcal/mol were submitted to SwissADME and assessed against the Lipinski and Veber rules, which flag oral drug-likeness and oral bioavailability respectively [14,27,28]. Eighteen compounds survived and were taken into ADMETlab 3.0 for ESOL solubility, cytochrome P450 liability, hERG inhibition and acute-toxicity class [15]. Seven cleared every filter.

2.10 Interaction analysis

Docked complexes for the seven finalists and for novobiocin were inspected in BIOVIA Discovery Studio Visualizer 2025 [22]. Hydrogen bonds, π-stacking and hydrophobic contacts were mapped and two-dimensional interaction diagrams exported.

3. Results

3.1 A homology model of mpox DNA topoisomerase 1B

SWISS-MODEL proposed four orthopox templates (vaccinia and variola, PDB IDs 4RVI, 6R8L, 3IGC and 2H7F), each sharing 40–45 % sequence identity with the mpox query and so comfortably above the 35 % threshold at which homology modelling becomes reliable [17]. The best of the four candidate models, built on 3IGC chain A (variola topoisomerase 1 in the transition state), returned a GMQE of 0.94 and a QMEANDisCo global score of 0.86 ± 0.05 and was taken forward (Figure 1).

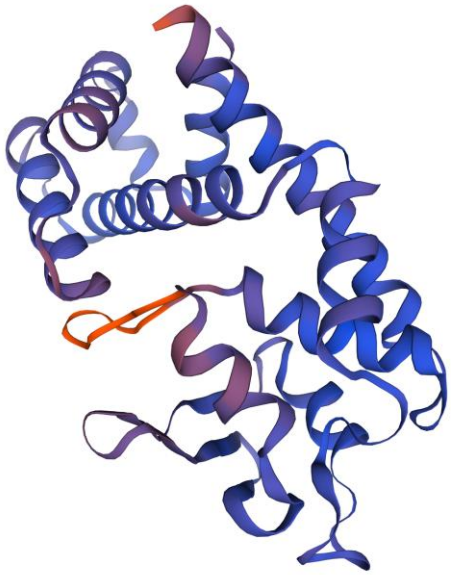
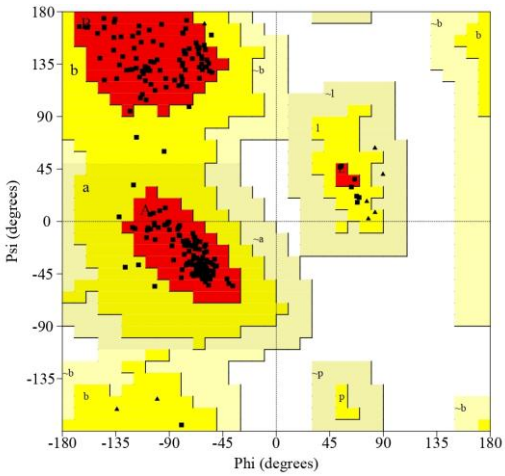
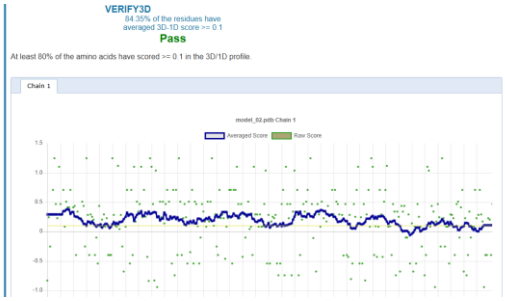


Figure 1. Ribbon representation of the mpox DNA topoisomerase 1B homology model, built on variola virus topoisomerase 1 in the transition state (PDB 3IGC, chain A).

3.2 Model validation

Validation on the SAVES v6.1 portal supported the model. PROCHECK placed 95.5 % of residues in favoured Ramachandran regions [19], VERIFY3D returned a pass with 84.35 % of residues scoring ≥ 0.1 [20], and the ERRAT overall quality factor was 95.1 % [21]. No chain breaks or steric clashes were found. Figure 2 shows the Ramachandran plot and the VERIFY3D profile.





(A) (B)

Figure 2. Stereochemical validation of the mpox Topo 1B homology model: (A) Ramachandran plot from PROCHECK; (B) VERIFY3D score profile.

3.3 Virtual screening

Docking the 1,353 phytochemicals produced 12,202 poses. Across the whole pose set the scores ran from −11.1 to −1.0 kcal/mol with a median of −6.2 kcal/mol; taking only the best pose per molecule, the range narrowed to −10.3 to −5.1 kcal/mol. Figure 3 shows the pose-level distribution. A retention threshold of −9.0 kcal/mol was set, slightly

more demanding than redocked novobiocin at −8.8 kcal/mol, and 113 unique compounds met it. That is a hit rate of 8 %, and these compounds went forward to ADMET profiling.

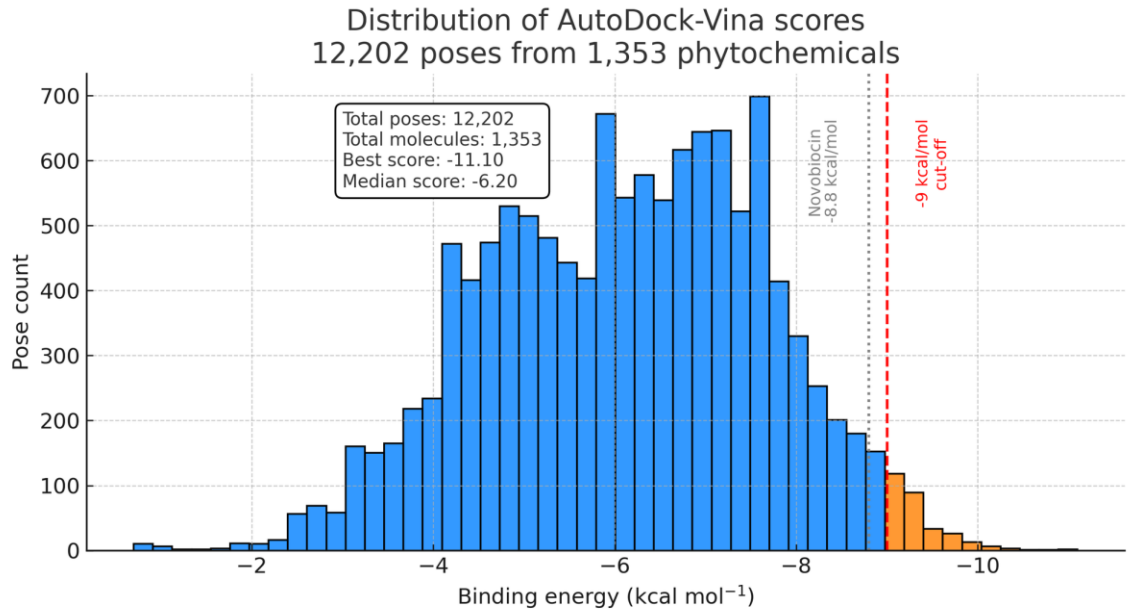
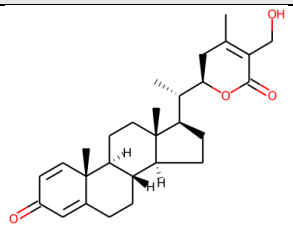
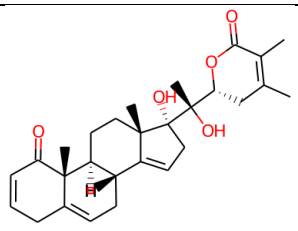


Figure 3. Distribution of AutoDock Vina scores over the 12,202 poses generated for 1,353 phytochemicals. The red dashed line marks the −9.0 kcal/mol retention threshold; the grey dotted line marks redocked novobiocin at −8.8 kcal/mol.

3.4 SwissADME and ADMETlab 3.0 profiling

Of the 113 docking hits, 18 satisfied every Lipinski and Veber criterion and were predicted to have high gastrointestinal absorption [14]. These 18 were carried into ADMETlab 3.0 for solubility, cytochrome P450, hERG and acute-toxicity checks [15], and seven cleared all of them. Withanolide L (IMPHY009438) was predicted moderately soluble and Withasomidienone (IMPHY000630) poorly soluble. Table 2 compares the seven finalists with novobiocin, and Tables 3 to 5 give the physicochemical, drug-likeness and ADMET detail.

Table 2. The seven ADMET-clean ligands, compared with the coumarin reference inhibitor novobiocin.

Compound	Structure	MW (Da)	Vina ΔG (kcal/mol)
Withasomidienone		438.60	−10.3
Withanolide L		452.58	−10.2

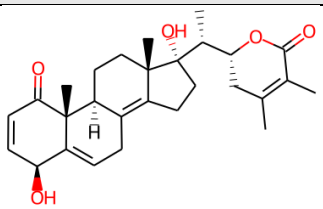
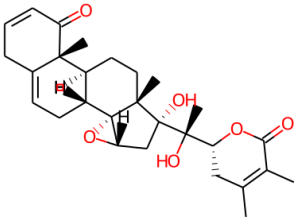
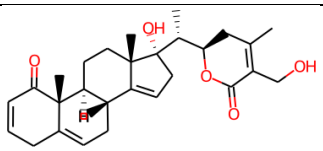
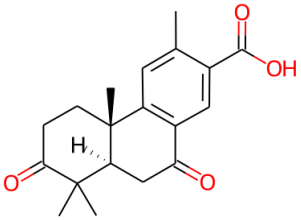
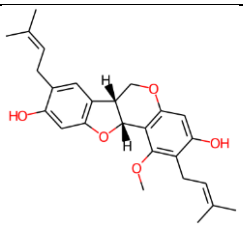
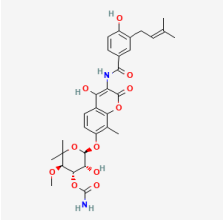
Compound	Structure	MW (Da)	Vina ΔG (kcal/mol)
Withanolide O		452.58	−9.9
Withanolide M		468.58	−9.8
Withanolide N		452.58	−9.6
Margolonone		314.38	−9.1
1-Methoxyficifolinol		422.51	−9.1
Novobiocin (reference)		612.65	−8.8

Table 3. Physicochemical descriptors for the shortlisted ligands. LogP and TPSA from SwissADME; identifiers from IMPPAT 2.0.

Compound	IMPPAT ID	HBD	HBA	MW (Da)	LogP	TPSA (Å²)
Withasomidienone	IMPHY000630	1	4	438.60	4.80	63.60
Withanolide L	IMPHY009438	2	5	452.58	3.66	83.83
Withanolide O	IMPHY005170	2	5	452.58	3.66	83.83
Withanolide M	IMPHY003143	2	6	468.58	3.31	96.36
Withanolide N	IMPHY005203	2	5	452.58	3.76	83.83

Compound	IMPPAT ID	HBD	HBA	MW (Da)	LogP	TPSA (Å²)
Margolonone	IMPHY013919	1	4	314.38	2.92	71.44
1-Methoxyficifolinol	IMPHY012575	2	5	422.51	4.44	68.15

Table 4. Drug-likeness profiles predicted by SwissADME. For the Lipinski filter, one violation or fewer is acceptable.

Compound	IMPPAT ID	Lipinski (viol.)	Ghose (viol.)	Veber	Egan	Muegge (viol.)
Withasomidienone	IMPHY000630	Passed (1)	Passed (0)	Bad	Bad	Bad (1)
Withanolide L	IMPHY009438	Passed (0)	Passed (0)	Good	Good	Good (0)
Withanolide O	IMPHY005170	Passed (0)	Passed (0)	Good	Good	Good (0)
Withanolide M	IMPHY003143	Passed (0)	Passed (0)	Good	Good	Good (0)
Withanolide N	IMPHY005203	Passed (0)	Passed (0)	Good	Good	Good (0)
Margolonone	IMPHY013919	Passed (0)	Passed (0)	Good	Good	Good (0)
1-Methoxyficifolinol	IMPHY012575	Passed (0)	Passed (0)	Good	Good	Bad (1)

Table 5. ADMET properties of the seven shortlisted ligands, predicted with SwissADME and ADMETlab 3.0. BBB = blood–brain barrier permeation; GI abs. = gastrointestinal absorption; Bioav. = bioavailability score; the columns headed 1A2 to 3A4 report predicted inhibition of the corresponding cytochrome P450 isoform; P-gp = P-glycoprotein substrate.

Compound	Solubility	BBB	GI abs.	Bioav.	1A2	2C19	2C9	2D6	3A4	P-gp
Withasomidienone	Poor	Yes	High	0.55	No	No	Yes	No	No	Yes
Withanolide L	Moderate	No	High	0.55	No	No	No	No	Yes	Yes
Withanolide O	Moderate	No	High	0.55	No	No	No	No	No	Yes
Withanolide M	Moderate	No	High	0.55	No	No	No	No	No	Yes
Withanolide N	Moderate	No	High	0.55	No	No	Yes	No	Yes	Yes
Margolonone	Soluble	No	High	0.85	No	No	No	No	No	Yes
1-Methoxyficifolinol	Poor	No	High	0.55	No	No	No	No	No	Yes

3.5 Topo 1B–ligand interactions

The seven finalists share a binding motif with two parts: a hydrogen-bond anchor to a polar residue, usually Lys133 or Lys167, and an aromatic clamp formed by Tyr136 and Tyr209 with hydrophobic support from the residues around them. Table 6 lists the contacts for each compound and Figure 4 shows the poses.

The hydrogen-bond network orients the ligands in the pocket. Withasomidienone, the top scorer, is anchored by conventional hydrogen bonds to the backbone of Lys133 and Gly132. Withanolide L reaches a stable pose instead through bonds to Lys167, Tyr136 and Tyr209, while Margolonone engages Thr142, Asn140 and Lys167. The identity of the polar partner therefore varies between scaffolds even though a polar anchor of some kind is present in six of the seven.

Non-polar contacts supply most of the remaining affinity. The aromatic side chain of Tyr136 forms π-stacking or π-alkyl interactions with the ligand core in every complex, and in several it is matched by a second aromatic contact from Tyr209 on the opposite face of the pocket. Arg130, Phe131 and Lys220 line the resulting cleft and pack against the non-polar faces of the steroid nucleus.

Novobiocin binds differently, which helps explain its weaker score. It makes several hydrogen bonds at the rim of the pocket, to Arg67, Asn140, Lys167 and Asp168, but does not reach Gly132 or Lys133. The rigid steroidal backbone

of the withanolides also fits the hydrophobic cleft more closely than the coumarin–noviose system of novobiocin, which accounts for the larger van der Waals term in their scores.

Table 6. Hydrogen-bond and hydrophobic or π-contacts observed for the seven ADMET-clean ligands and for novobiocin docked to mpox DNA topoisomerase 1B.

Compound	**Hydrogen bond(s)**	**Hydrophobic / π-contacts**
Withasomidienone	Lys133, Gly132	Tyr136, Thr142, Lys167, Arg130, Asn140
Withanolide L	Lys167, Tyr136, Tyr209	Arg130, Lys220, Arg67, Thr142
Withanolide O	Lys167	Tyr136, Lys220, Arg130, Phe131, Thr142
Withanolide M	Lys167	Tyr136, Arg218, Phe131
Withanolide N	—	Tyr136, Arg130, Phe131, Ile219
Margolonone	Thr142, Asn140, Lys167	Tyr136, Arg130, Gly132, Lys133, Phe131
1-Methoxyficifolinol	Tyr209, Lys220	Tyr209, Arg218, Ile219, Lys133
Novobiocin	Arg67, Asn140, Lys167, Asp168	Tyr136, Arg130, Phe131, Arg218, Lys220, Ile219

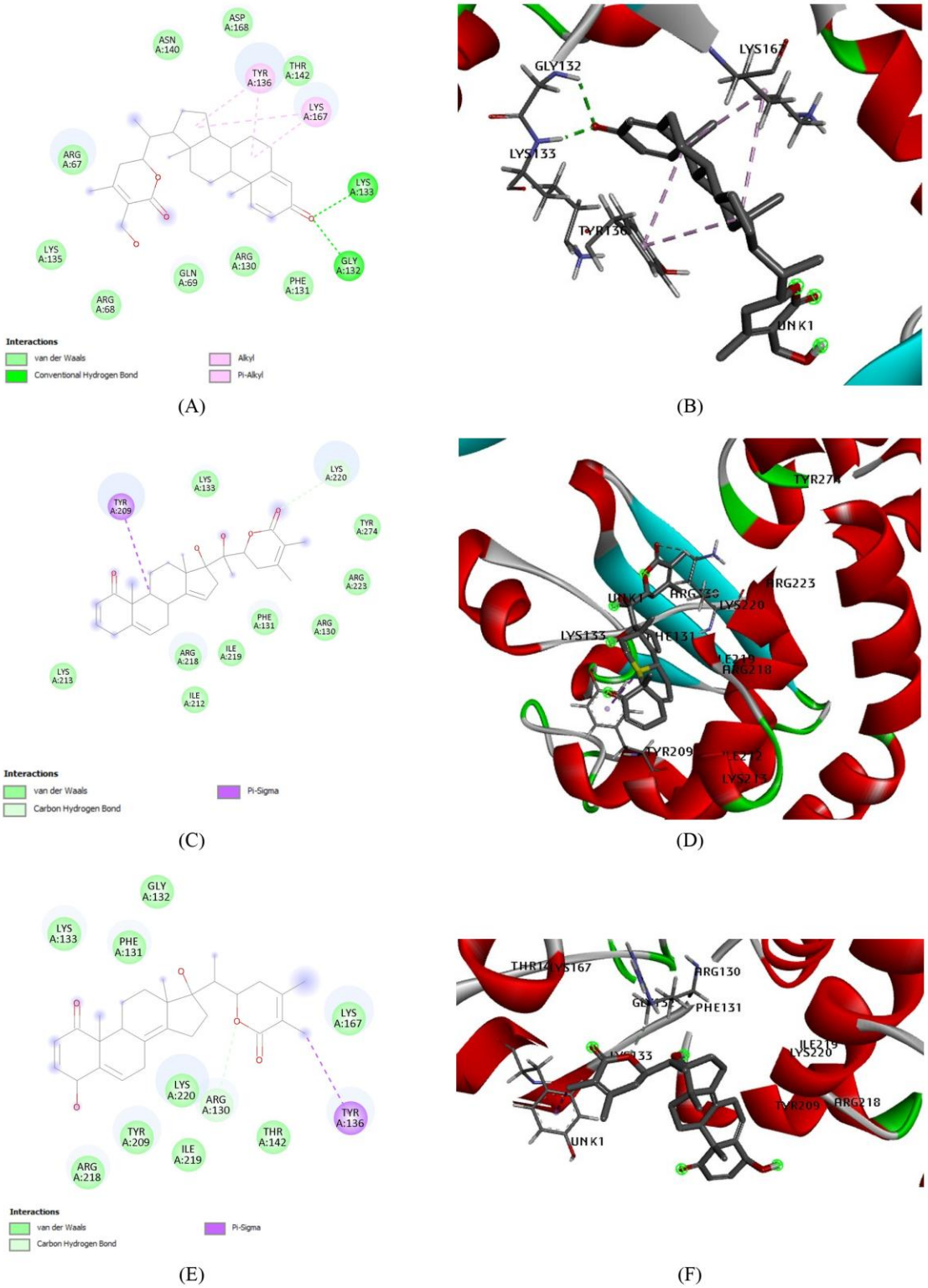
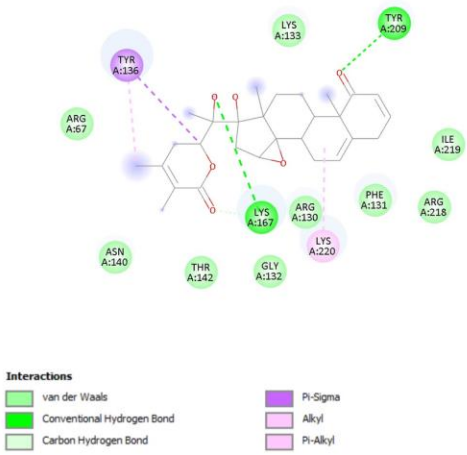
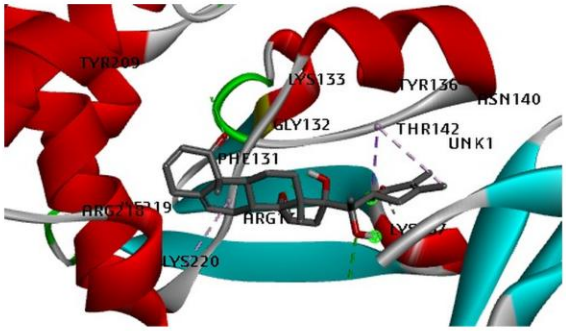


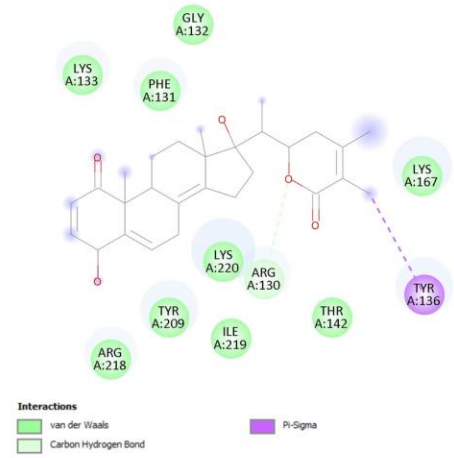
Figure 4. Binding modes of the lead candidates in the mpox Topo 1B pocket, shown as two-dimensional interaction diagrams paired with the corresponding three-dimensional pose: (A, B) Withasomidienone; (C, D) Withanolide L; (E, F) Withanolide O. Panels (G) to (P) continue overleaf.



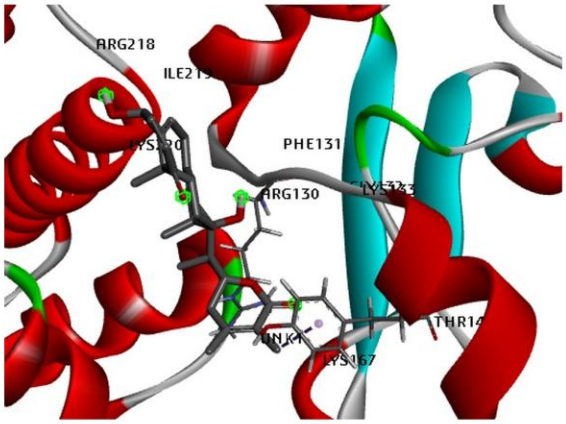
(G)



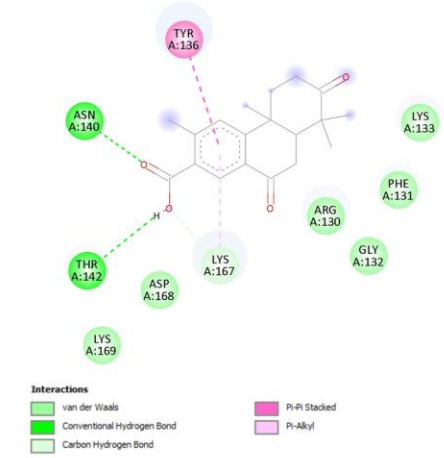
(H)



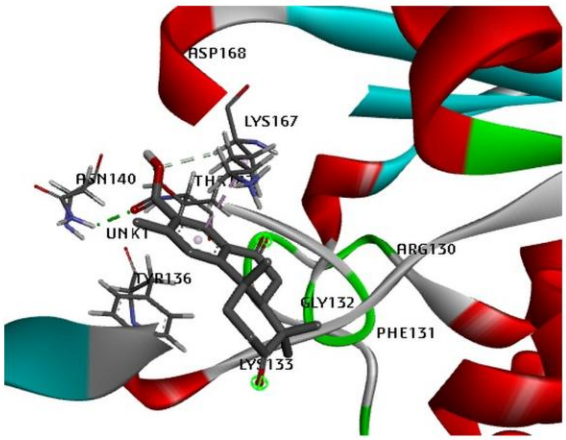
(I)



(J)



(K)



(L)

Figure 4 (continued). (G, H) Withanolide M; (I, J) Withanolide N; (K, L) Margolonone.

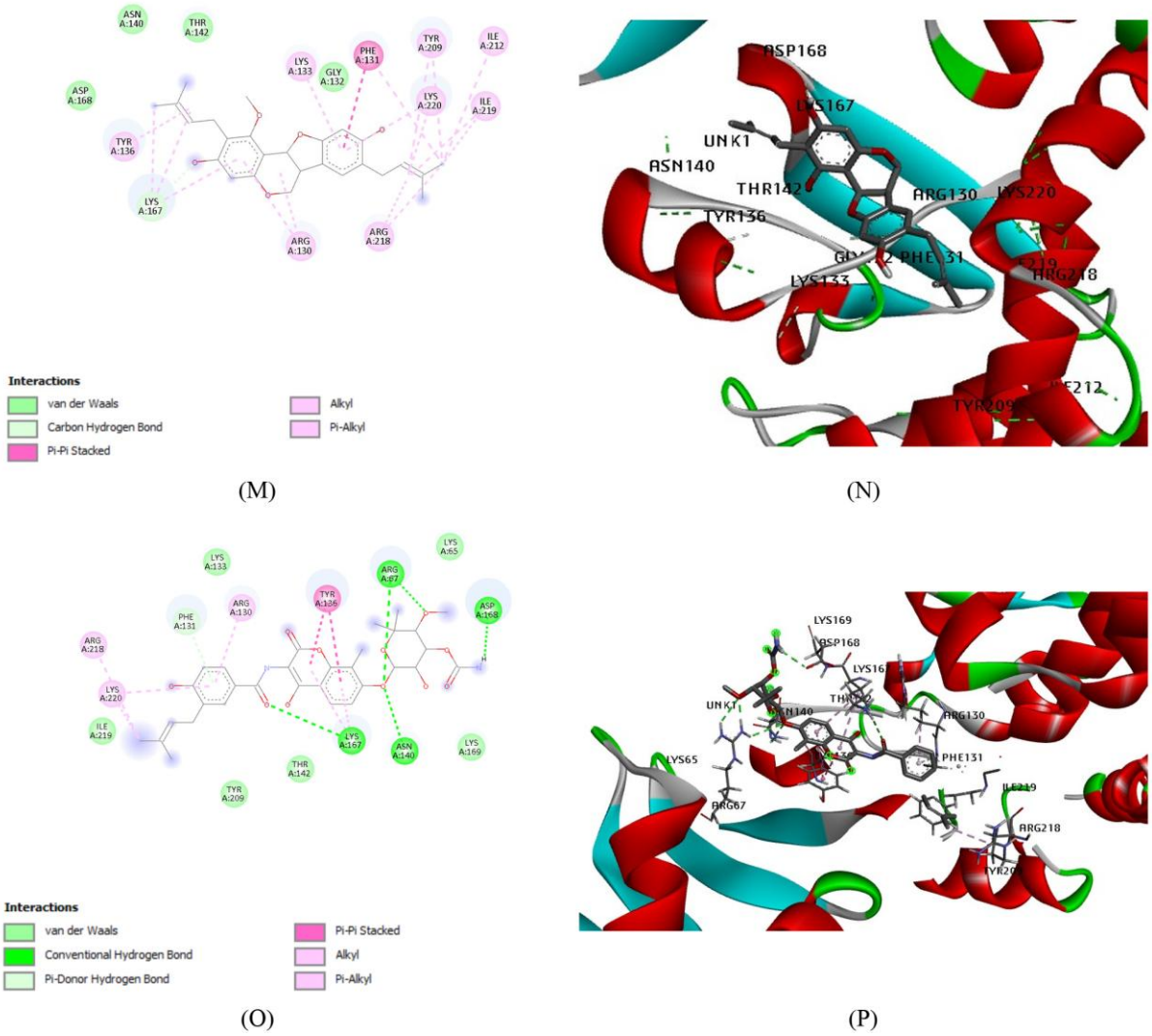


Figure 4 (continued). (M, N) 1-Methoxyficifolinol; (O, P) novobiocin, the reference inhibitor.

4. Discussion

Resistance to tecovirimat and the toxicity ceiling on brincidofovir between them leave mpox with no comfortable second line, which is the practical case for screening against a different enzyme [29]. Topo 1B suits that purpose: it is essential for orthopoxvirus replication and its identity with human TOP1 stays below 45 %, so selective inhibition is at least structurally plausible [7,17]. Screening 1,353 phytochemicals from 16 Indian medicinal plants against a validated model of the enzyme returned seven compounds scoring between −9.1 and −10.3 kcal/mol, all of which beat redocked novobiocin and none of which carried a predicted hERG, P450 or acute-toxicity flag. Five are withanolides from *Withania somnifera*, a genus with reported activity against dengue and influenza virus [9].

Choosing between the top two hits was the main judgement call in the study. Withasomidienone scored 0.1 kcal/mol better than Withanolide L, a gap far inside Vina's 2–3 kcal/mol error band and not a basis for ranking anything [11,30]. Withasomidienone is also predicted poorly soluble and breaks one Lipinski rule, while Withanolide L is predicted moderately soluble with no violations. Since poor aqueous solubility is one of the commonest reasons compounds fail late [31], we advanced Withanolide L and kept Withasomidienone as a potency reserve.

Several limitations bound these conclusions. Docking scores of this kind carry a mean error of roughly 2–3 kcal/mol, so the ordering within the shortlist should be read as a grouping rather than a ranking [11,30]. The receptor was held rigid, so induced fit is not represented, and the target itself is a homology model rather than an experimental structure: the fold and the pocket residues are well supported by the templates, but side-chain positions in the pocket are inferred. The ADMET numbers come from QSAR models whose accuracy drops for scaffold classes thinly represented in their training sets, and withanolides are not a large class in those sets [14,15]. Nothing here has been tested against the enzyme.

The experimental path from here is short and well defined. Molecular dynamics over 100–200 ns on the top complexes would admit protein flexibility and allow MM/GBSA or MM/PBSA rescoring, which usually separates a shortlist better than docking alone [32]. Enzymatic assays against recombinant orthopox Topo 1B would then give IC_{50} values, and surface plasmon resonance or isothermal titration calorimetry would supply dissociation constants and association and dissociation rates [16]. Aqueous solubility and microsomal stability assays would test the two ADMET predictions that drove the lead choice. Whether Withanolide L and its analogues deserve the label of preclinical leads depends on those measurements.

5. Conclusion

Homology modelling, a 1,353-compound virtual screen and a two-stage ADMET funnel together identified seven phytochemical scaffolds that dock to mpox DNA topoisomerase 1B more tightly than novobiocin and carry no predicted safety flag. Withanolide L (IMPHY009438) is the front-runner, on a combination of −10.2 kcal/mol predicted affinity, moderate predicted solubility and no Lipinski violations rather than on score alone. Withasomidienone is retained as a potency reserve.

These are predictions. Confirming them needs molecular dynamics with MM/PBSA or MM/GBSA rescoring, enzymatic IC_{50} determination against recombinant orthopox Topo 1B, and measured solubility and metabolic stability [15,16,32]. If those hold, the scaffolds reported here would act on a target orthogonal to F13 and could complement tecovirimat rather than replace it, which matters while resistant strains continue to appear [2,3]. The wider point is unchanged by this study but supported by it: ethnopharmacological chemical space still holds usable starting material for antiviral programmes [33,34].

Declarations

Funding. The authors received no financial support for the research, authorship or publication of this article.

Competing interests. The authors declare that they have no competing financial or non-financial interests.

Author contributions. Tanya Jindal and Isha Thakur performed the computational work. Tanya Jindal, Isha Thakur and Gurinder Singh prepared the manuscript. Puneet reviewed and proofread the manuscript. Harpreet Kaur provided the computational infrastructure. All authors read and approved the final manuscript.

Data availability. All phytochemical structures used in this study are publicly available from the IMPPAT 2.0 atlas (https://cb.imsc.res.in/imppat/). The homology model, docking configuration files and the complete score table are available from the corresponding author on reasonable request.

Ethics approval. Not applicable. This study did not involve human participants, human material or animals.

References

1. World Health Organization. Multi-country outbreak of mpox: external situation report no. 53, 29 May 2025. Geneva: World Health Organization; 2025. Available from: https://www.who.int/publications/m/item/multi-country-outbreak-of-mpox--external-situation-report--53---29-may-2025

2. Smith TG, Gigante CM, Wynn NT, Matheny A, Davidson W, Yang Y, et al. Tecovirimat resistance in mpox patients, United States, 2022–2023. Emerg Infect Dis. 2023;29(12):2518–25.

3. Peng Y, Guo Y, Li X, Zhang Y, Wang Q, Li J, et al. Structural insights into tecovirimat antiviral activity and mechanisms of poxvirus resistance. Nat Microbiol. 2025;10(1):1–12.

4. National Institute of Diabetes and Digestive and Kidney Diseases. Brincidofovir. In: LiverTox: clinical and research information on drug-induced liver injury. Bethesda (MD): NIDDK; 2022. Available from: https://www.ncbi.nlm.nih.gov/books/NBK585270/

5. Russo AT, Grosenbach DW, Chinsangaram J, Honeychurch KM, Long PG, Lovejoy C, et al. Antivirals with activity against mpox: a clinically oriented review. Clin Infect Dis. 2023;76(1):155–64.

6. Franke BW, Hruby DE. Poxvirus DNA topoisomerase knockout mutant exhibits decreased viability. J Virol. 1996;70(8):5640–4.

7. Sekiguchi J, Shuman S. Mechanism of inhibition of vaccinia DNA topoisomerase by the coumarin antibiotic novobiocin. J Biol Chem. 1996;271(2):938–44.

8. Wittschieben J, Shuman S. Mechanism of DNA transesterification by vaccinia topoisomerase: catalytic contributions of lysine-167, aspartate-221 and aspartate-266. J Biol Chem. 1997;272(29):18250–7.

9. Den Haan H, de Jong W, van der Vliet K, Meijer A, van Kuppeveld FJM. Natural products as antiviral agents. Front Microbiol. 2020;11:568.

10. Mohanraj K, Karthikeyan BS, Vivek-Ananth RP, Chand RPB, Aparna SR, Mangalapandi P, et al. IMPPAT 2.0: an enhanced and expanded phytochemical atlas of Indian medicinal plants. ACS Omega. 2023;8(11):10543–51.

11. Trott O, Olson AJ. AutoDock Vina: improving the speed and accuracy of docking with a new scoring function, efficient optimization and multithreading. J Comput Chem. 2010;31(2):455–61.

12. Dallakyan S, Olson AJ. Small-molecule library screening by docking with PyRx. Methods Mol Biol. 2015;1263:243–50.

13. Eberhardt J, Santos-Martins D, Tillack AF, Forli S. AutoDock Vina 1.2.0: new docking methods, expanded force field and Python bindings. J Chem Inf Model. 2021;61(8):3891–8.

14. Daina A, Michielin O, Zoete V. SwissADME: a free web tool to evaluate pharmacokinetics, drug-likeness and medicinal chemistry friendliness of small molecules. Sci Rep. 2017;7:42717.

15. Fu L, Shi S, Yi J, Wang N, He Y, Wu Z, et al. ADMETlab 3.0: an updated comprehensive online ADMET prediction platform. Nucleic Acids Res. 2024;52(W1):W422–31.

16. Hu X, An S, Chu J, Liang B, Liao Y, Jiang J, et al. Potential inhibitors of monkeypox virus revealed by molecular modeling approach to viral DNA topoisomerase I. Molecules. 2023;28(3):1444.

17. Waterhouse A, Bertoni M, Bienert S, Studer G, Tauriello G, Gumienny R, et al. SWISS-MODEL: homology modelling of protein structures and complexes. Nucleic Acids Res. 2018;46(W1):W296–303.

18. UCLA-DOE Institute. SAVES v6.1: structure validation server. Available from: https://saves.mbi.ucla.edu/

19. Laskowski RA, MacArthur MW, Moss DS, Thornton JM. PROCHECK: a program to check the stereochemical quality of protein structures. J Appl Crystallogr. 1993;26(2):283–91.

20. Lüthy R, Bowie JU, Eisenberg D. Assessment of protein models with three-dimensional profiles. Nature. 1992;356(6364):83–5.

21. Colovos C, Yeates TO. Verification of protein structures: patterns of nonbonded atomic interactions. Protein Sci. 1993;2(9):1511–9.

22. BIOVIA, Dassault Systèmes. BIOVIA Discovery Studio Visualizer, version 2025. San Diego (CA): Dassault Systèmes; 2025.

23. Morris GM, Huey R, Lindstrom W, Sanner MF, Belew RK, Goodsell DS, et al. AutoDock4 and AutoDockTools4: automated docking with selective receptor flexibility. J Comput Chem. 2009;30(16):2785–91.

24. Jendele L, Krivák R, Škoda P, Novotný M, Hoksza D. PrankWeb: a web server for ligand binding site prediction and visualization. Nucleic Acids Res. 2019;47(W1):W345–9.

25. O'Boyle NM, Banck M, James CA, Morley C, Vandermeersch T, Hutchison GR. Open Babel: an open chemical toolbox. J Cheminform. 2011;3:33.

26. Feinstein WP, Brylinski M. Calculating an optimal box size for ligand docking and virtual screening against experimental and predicted binding pockets. J Cheminform. 2015;7:18.

27. Lipinski CA, Lombardo F, Dominy BW, Feeney PJ. Experimental and computational approaches to estimate solubility and permeability in drug discovery and development settings. Adv Drug Deliv Rev. 2001;46(1–3):3–26.

28. Veber DF, Johnson SR, Cheng HY, Smith BR, Ward KW, Kopple KD. Molecular properties that influence the oral bioavailability of drug candidates. J Med Chem. 2002;45(12):2615–23.

29. Saeed S, St-Denis A, Andronescu M, Hoang L, Morshed M, Fraser E, et al. Tecovirimat-resistant mpox cluster — British Columbia, Canada, 2024. MMWR Morb Mortal Wkly Rep. 2024;73(40):883–7.

30. Koes DR, Baumgartner MP, Camacho CJ. Lessons learned in empirical scoring with smina from the CSAR 2011 benchmarking exercise. J Chem Inf Model. 2013;53(8):1893–904.

31. Savjani KT, Gajjar AK, Savjani JK. Drug solubility: importance and enhancement techniques. ISRN Pharm. 2012;2012:195727.

32. Genheden S, Ryde U. The MM/PBSA and MM/GBSA methods to estimate ligand-binding affinities. Expert Opin Drug Discov. 2015;10(5):449–61.

33. Newman DJ, Cragg GM. Natural products as sources of new drugs over the nearly four decades from 01/1981 to 09/2019. J Nat Prod. 2020;83(3):770–803.

34. Mani JS, Johnson JB, Steel JC, Broszczak DA, Neilsen PM, Walsh KB, et al. Natural product-derived phytochemicals as potential agents against coronaviruses and other viruses: a review. Front Microbiol. 2020;11:1996.